Enhancement of Thermoelectric Efficiency of MnSi$_{1.75}$ with the Addition of Externally Processed Nanostructured MnSi

Xinghua Shi, Zahra Zamanipour, Kenneth F. Ede, Jerzy S. Krasinski, Daryoosh Vashaee[*]
Helmerich Advanced Technology Research Center, Oklahoma State University, Tulsa, OK 74106, USA
[*]daryoosh.vashaee@okstate.edu

Abstract – Higher manganese silicide is one of the promising thermoelectric materials for waste heat recovery at medium temperature (500-700 °C). Improvement on thermoelectric performance of bulk thermoelectric higher manganese silicide MnSi$_{1.75}$ is introduced by externally mixing 1 at% nanostructured MnSi to MnSi$_{1.75}$. This method can reduce the thermal conductivity above 400 °C more than reducing the power factor of the higher manganese silicide. This would enhance the figure-of-merit ZT of MnSi$_{1.75}$ to ZT≅0.5 without any doping at 570 °C. In comparison, the figure-of-merit of conventional MnSi$_{1.75}$ is ZT≅0.3. This method can be easily applied to industrial manufacturing of this material to enhance its efficiency.

Keywords- thermoelectric, higher manganese silicide, nanostructuring, MnSi

I. INTRODUCTION

As the Earth's population continues to grow, the demand for energy is rapidly increasing. Furthermore, due to global environmental concerns, a constant increase in fuel prices, and the threat of fossil fuels depletion, has created a market for alternative energy. The development of clean, recycled, environmentally friendly and low-cost energy sources is necessary. Thermoelectric (TE) generators can convert waste heat energy into electricity. With about 60% of the world's useful energy wasted as heat, TE offers useful means to recycle and convert large amounts of waste energy to electricity.

For TE green applications, the most well-known thermoelectric materials are based on groups IV and V chalcogenides. However, these groups present two major drawbacks; cost and toxicity. In contrast, Mn and Si, the two abundant elements in Earth's crust, are non-toxic. Higher Manganese Silicide (HMS) is a good candidate to make low-cost thermoelectric materials with low-environmental load [1] for medium to high temperature (500ºC-700ºC) applications. The development of high performance thermoelectric generators for this range of temperature is highly desired [2]. In addition, HMS offers a low vapor pressure, strong hardness and high resistance to oxidation with atmospheric oxygen. One of the most immediate large scale applications of HMS is in automobiles. In most au-

tomobiles, more than 70 percent of the fuel's energy is wasted as heat. Thermoelectric generators can be used to recover waste heat from the engine and increase the fuel efficiency.

Alloys of Silicon and Manganese with higher composition of Si such as Mn$_{11}$Si$_{19}$, Mn$_{15}$Si$_{26}$, Mn$_{27}$Si$_{47}$ and Mn$_4$Si$_7$ are p-type semiconductors with almost similar thermoelectric properties. They all make Chimney-ladder structures with an energy gap of approximately 0.7 eV. HMS compounds may contain nano to micro scale regions of manganese monosilicide (MnSi). These compounds have been attractive to researchers seeking to optimize such features in order to reduce the thermal conductivity of the compound [3-6]. Though the presence of the MnSi phase in the HMS matrix is virtually unavoidable, the TE performance of HMS can be improved by alternative synthesis methods that control the distribution pattern and size of the MnSi phase such as in the case when MnSi is dispersed in the matrix in nanostructured form. Higher manganese silicide with in-situ formed nano-phase of MnSi has been proven to get high thermoelectric performance using a rapid melt-spinning process combined with a spark plasma sintering method [7]. However, the method involves a complicated process and relatively high experimental conditions. The main drawback is the slow rate of HMS production for the manufacturing industry.

Researchers usually add other elements to enhance ZT. Ge [5] is the typical choice. But high purity Ge is expensive and it easily oxidizes. As mentioned previously Mn and Si are inexpensive and abundant elements. Additionally, MnSi has metallic properties and high resistance to oxidation. Initially, we externally added a small amount (~1 at.%) of nanostructured MnSi into higher manganese silicides' matrix. Our findings demonstrated that it is a relatively quick, low-cost and scalable method for the inclusion of MnSi nano-phase compared to others methods.

II. METHODOLOGY

The HMS powder was prepared from 100 mesh silicon and 325 mesh manganese powders obtained from Alfa Aesar Co. with purity of 99.9% and 99.99%, respectively. The amount of each component was weighed in an argon-filled glove box for different compositions of MnSi$_x$ with x= 1.75 and x=1. The mixed powder and tungsten carbon

balls were loaded under argon atmosphere in tungsten carbide bowls with ball to powder weight ratio (BPR) of 5. The bowls were hermetically sealed and were loaded in a planetary ball mill. Fritsch's planetary ball mills P6 (for $MnSi_{1.75}$) and P7PL (for MnSi) with the maximum speed of 650 rpm and 1000 rpm, respectively, were used (i.e. equal to centrifugal acceleration of about 29G and 85G, respectively. G is gravitational constant). The mixed nano-structured $MnSi_{1.75}$ and MnSi powders were heat treated at 1050 °C and 1200 °C in a muffled furnace under argon atmosphere, respectively.

The powder was weighted and loaded into a graphite die with inner diameter of 12.7 mm. All samples were sintered under 108 MPa pressure at 950°C for 0-4 minutes. The sintered samples were cut into disks and rods for different characterizations. The thermal conductivity was measured by a laser flash apparatus (Netzsch LFA 457 Micro Flash). The Seebeck coefficient and electrical resistivity were measured simultaneously using a commercial apparatus (Ulvac-Riko's ZEM-3). X-ray diffraction analysis and scanning electron microscopy were performed using Bruker AXS D8 with Cu Kα radiation and Hitachi S-4800, respectively.

III.   EXPERIMENTAL DATA

In order to determine how the composite of MnSi affects the $MnSi_{1.75}$ TE properties, we prepared reference $MnSi_{1.75}$ powder by mechanical alloying and without any doping to use as a benchmark. Mechanical alloying can produce purer higher manganese silicide than the other methods involving heat treatments. Through this conventional preparation process, relatively pure $MnSi_{1.75}$ phase can be formed by high energy ball milling. We also tried melting and heat treatment of powders to produce the HMS alloy for comparison. Nanostructured MnSi powder was pre-pared by using a combination of mechanical milling and heat treatment of the mixed powder at 1200 °C. Further-more, 1 at.% nanostructured MnSi powder was mixed with the reference $MnSi_{1.75}$ powder by ball milling. We col-lected XRD patterns and compared the two kinds of higher manganese silicide powders. The results are shown in Fig. 1(a). The bottom (black) curve shows the XRD pattern of the reference $MnSi_{1.75}$ powder and the top (red) curve shows that of the reference $MnSi_{1.75}$ powder mixed with 1 at.% nanostructured MnSi powder. According to Figure 1, there is no MnSi in the reference $MnSi_{1.75}$ powder. How-ever, there is a small MnSi peak in $MnSi_{1.75}$+MnSi powder (which may be difficult to see in the figure). The HMS lines are also shown in Figure 1 with no Mn or Si line indicating that the alloying is complete within the accuracy of the XRD analysis.

From each powder, we sintered a bulk sample. The sam-ples were sintered by hot pressing under same conditions. The heat was produced by joule heating the sample utiliz-ing running DC current through the sample. In order to avoid the grain growth of MnSi during sintering, the heat-ing current was immediately turned off after the sample reached at 950°C. The XRD patterns of the two HMS samples were collected and compared in Fig. 1(b). The bottom (black) XRD pattern belongs to the HMS sample made of the reference $MnSi_{1.75}$, and the top (red) XRD pattern belongs to the HMS sample made of $MnSi_{1.75}$

mixed with 1 at.% nanostructured MnSi powder. After sintering, a small MnSi phase was observed in the refer-ence sample. However, the MnSi peak in $MnSi_{1.75}$+MnSi sample is relatively stronger indicating its higher content.
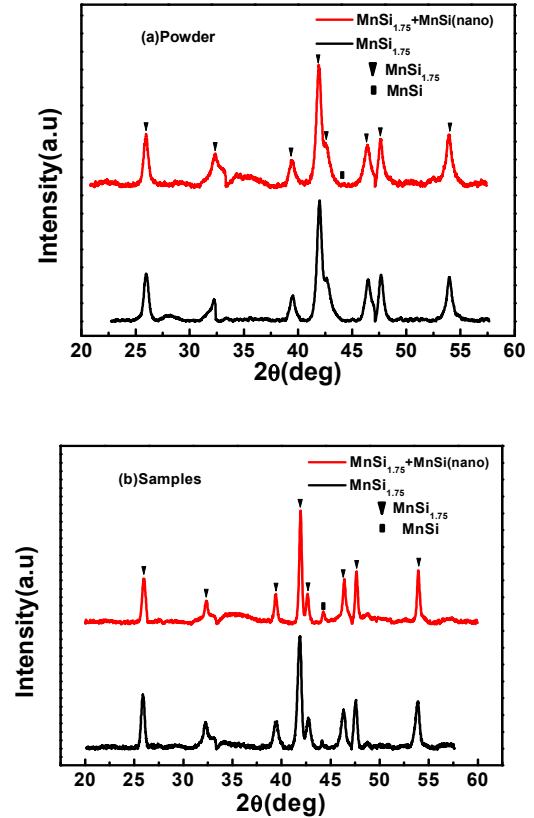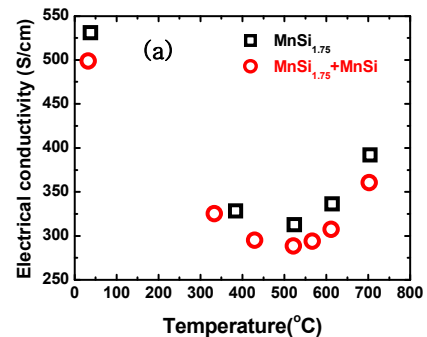

Figure 1: XRD patterns of (a) the reference $MnSi_{1.75}$ powder (bottom-black) and $MnSi_{1.75}$ mixed with 1 at.% nanostructured MnSi powder (top-red), and (b) the reference $MnSi_{1.75}$ bulk sample (bottom-black) and $MnSi_{1.75}$ mixed with 1 at.% nanostructured MnSi sample (top-red).

The MnSi content in the reference sample may be asso-ciated with localized variation of stoichiometry in the sample. In contrast, the MnSi phase in $MnSi_{1.75}$+MnSi sample is uniformly dispersed by prior ball milling of the mixed powder.

IV.   RESULTS AND DISCUSSION

Fig. 2(a) shows the electrical conductivity of the bulk samples. The squared curves describe the properties of the reference sample and the circled curves describe the prop-erties of $MnSi_{1.75}$+MnSi sample.

Figure labels (Fig. 2): (b) Seebeck coefficient (μV/K), MnSi$_{1.75}$ (squared), MnSi$_{1.75}$+MnSi (circled); (c) Power Factor, PFT (W/mK); (d) Thermal conductivity (W/mK); (e) Figure-of-merit, ZT; x-axis Temperature(°C).
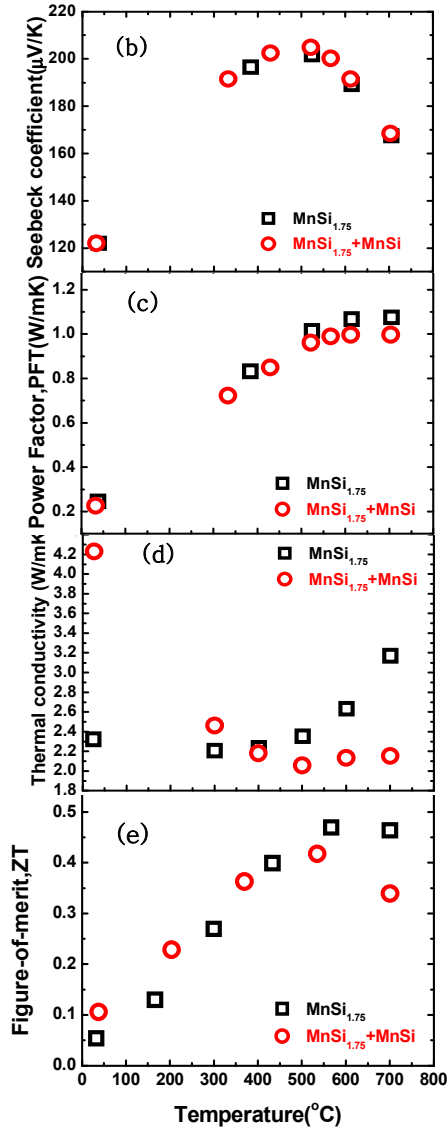
Figure 2: Temperature dependence of (a) electrical conductivity, (b) Seebeck coefficient, (c) power factor times temperature, (d) thermal conductivity, and (e) figure-of-merit ZT of the reference MnSi$_{1.75}$ (squared) and MnSi$_{1.75}$ + MnSi (circled) samples.

The temperature dependence of electrical conductivities demonstrates a metallic or degenerate electrical conduction. The electrical conductivities of the two samples have only a small difference. In fig. 2(b), the Seebeck coefficients versus temperature show similar values. The Seebeck coefficient increases with temperature up to 550 °C, and decreases at T>550 °C owing to the excitation of intrinsic carriers. The temperature dependences of power factor are also similar as expected because the electrical conductivity and Seebeck coefficient of the two samples are similar. Fig. 2(c) gives temperature dependence of power factor. The reference MnSi$_{1.75}$ sample and MnSi$_{1.75}$ mixed with 1 at.% nanostructured MnSi sample trends are very similar. However, the temperature dependences of thermal conductivities for the two samples are obviously different in Fig. 2(d). The thermal conductivity of the reference MnSi$_{1.75}$ sample decreases with temperature up to 500 °C and rapidly increases with temperature at T>500 °C, which is attributed to the ambipolar thermal diffusion. [8] In contrast, the thermal conductivity of the MnSi$_{1.75}$+MnSi sample decreases up to 500 °C and increases only slowly at T>500 °C compared with that of the reference sample. This value is even smaller than previously reported small thermal conductivity for MnSi$_{1.73}$ [9]. This is mainly due to the presence of the MnSi nano-phase that is evenly distributed in the HMS matrix. Due to the greatly increased density of interfaces at MnSi grain boundaries, phonons are significantly scattered reducing the lattice part of thermal conductivity. Moreover, since the thermal conductivity remains low at high temperature, it indicates that the ambipolar thermal diffusion is considerably suppressed. This suppression can be due to the fact that the grain boundaries scatter electrons, which are thermally excited, more than holes due to the electrons' smaller energy.

Fig. 2(e) shows the temperature dependence of the dimensionless figure-of-merit ZT for the same two samples. Since the power factor of the two samples is similar, the reduction of the thermal conductivity in MnSi$_{1.75}$+MnSi sample leads to the enhancement of ZT at high temperature (400-700 °C).

V.   CONCLUSION

In summary, we demonstrated that adding a small amount (~1 at.%) of nanostructured MnSi to MnSi1.75 reduces both lattice and ambipolar parts of thermal conduction by scattering of phonon and minority carriers more than majority ones, respectively. Thus, the thermoelectric figure-of-merit ZT at high temperature is enhanced and the efficiency of the relevant device can be improved. This effect may prove to be a stepping stone for further enhancing thermoelectric properties of HMS by optimizing the amount of nanostructured MnSi in the matrix.

REFERENCES

[1] B. Poudel, Q. Hao, Y. Ma, Y. Lan, A. Minnich, B. Yu, X. Yan, D. Wang, A. Muto, D. Vashaee, X. Chen, J. Liu, M. S. Dresselhaus, G. Chen, Z. Ren, "High-Thermoelectric Performance of Nanostructured Bismuth Antimony Telluride Bulk alloys," Sci., 320. no. 5876, pp. 634 – 638, 2008.

[2] A. J. Minnich, X. Wang, H. Lee,1 M. S. Dresselhaus, Z.F. Ren, G. Chen, and D. Vashaee, "Modeling study of thermoelectric SiGe nanocomposites," Phys. Rev. B., vol. 80, pp. 15, 2009.

[3] D.M. Rowe, CRC handbook of thermoelectric, Boca Raton, FL: CRC Press LLC, 1995.

[4] M. C. Bost and J. E. Mahan, " An Optica Determination of the Bandgap of the Most Silicon-Rich Manganese Silicide Phase," J. Elec. Mater., vol. 16, pp. 6, 1987.

[5] A. J. Zhou, T. J. Zhu, X. B. Zhao, S. H. Yang, T. Dasgupta, C. Stiewe, R. Hassdorf, and E. Mueller, "Improved Thermoelectric Performance of Higher Manganese Silicides with Ge Additions," J. Elec. Mater., vol. 39, pp. 9, 2009.

[6] K. Kakubo, Y. Kimura and Y. Mishima, "Microstructures and thermoelectric power of the higher manganese silicide alloys," Mat. Res. Soc. Symp. Proc. 646, 2001.

[7] W. Luo, H. Li, Y. G.Yan, Z. B. Lin, X. F. Tang, Q. J. Zhang and C. Uher, "Rapid Synthesis of high thermoelectric performance higher manganese silicide with in-situ formed nano-phase of MnSi," Inte., vol. 19, pp. 404, 2011.

[8] F. E. Geiger, F. G. Cunningham, "Ambipolar Diffusion in semiconductors," Amer. J. Phys., vol. 32, 5, pp. 336-342, 1964.

[9] I. Aoyama, H. Kaibe, L. Rauscher, T. Kanda, M. Mukoujima, S. Sano and T. Tsuji, "Doping Effects on Thermoelectric Properties of Higher Manganese Silicides (HMSs, MnSi1.74) and Characterization of Thermoelectric Generating Module using P-Type (Al, Ge and Mo)-doped HMSs and n-Type Mg2Si0.4Sn0.4 Legs," Jpn J. Appl. Phys., vol. 44, pp. 4275, 2005.